DYNAMICS OF PARTICLES ON INTERFACES
AND IN THIN LIQUID FILMS

Jordan T. Petkov, Nikolai D. Denkov

Laboratory of Chemical Physics and Engineering, Faculty of Chemistry

Sofia University, 1164 Sofia, Bulgaria

1. INTRODUCTION.

The invention of uniformly sized, polymer micro-spheres in 1950s provided the possibility for a direct optical observation of various equilibrium structures and dynamic processes in two dimensions (2D). These include 2D-phase transitions, particle aggregation, deposition on solid surfaces, fracture of 2D particulate layers, and many others. The initial interest was driven mainly by the possibility for direct observation and precise quantitative analysis of these complex phenomena, which include many-body interactions and are of great interest for the condensed matter physics. The optical observations have been often combined with computer experiments, in which the collective properties of the particles are simulated. During the last decade, the research interest shifted to a large extend towards the mechanisms and procedures for controlled fabrication of new 2D-structured materials, which possess unique optical properties and has a potential for various applications in nanotechnology.

The purpose of this paper is to present a brief overview of several research areas where the dynamics of colloid particles in two dimensions is studied. The review covers the following topics: determination of the rheological properties (surface viscosity and yield stress) of adsorption surfactant layers and lipid vesicles by studying the dynamics of single particles; aggregation and ordering of particles on surfaces and in thin films (2D fractals, colloid crystals and phase transitions); mechanism of particle deposition on solid surfaces in evaporating layers (preparation of structured nano-materials, painting); effect of particles on the stability of liquid films (oscillatory structure forces, antifoaming). Since the available

space is restricted, we present only the main ideas and conclusions with emphasis on the relations between the different areas. For details, the reader is referred to the original papers.

First, we briefly introduce the basic terms, which are used to describe the configuration of solid particles attached to an interface or captured in a liquid film. The three-phase contact angle, α (see Fig. 1A), is experimentally measurable quantity, which brings information about the interfacial energies of the contacting phases [1-3]. According to the Young equation, the equilibrium contact angle measured through phase 2, α_2, can be expressed as

$$\cos\alpha_2 = (\sigma_{13} - \sigma_{12})/\sigma_{23} \tag{1}$$

where σ_{ik} is the energy per unit area of the interface formed between phases i and k. For the fluid interface (formed between phases 2 and 3), σ_{23} is equal to the interfacial tension, which can be measured by various methods [1]. On the other side, the direct determination of the solid-fluid interfacial energies, σ_{12} and σ_{13}, is a difficult task, and the contact angle measurement is one way to gain information about them [1-3]. We refrain from discussing here all complications related to the differences between the equilibrium, receding and advancing contact angles (viz. the contact angle hysteresis), as well as the specific difficulties in the contact angle measurements with solid surfaces, because these are very wide topics, which are beyond the scope of the paper (see e.g. refs. [2, 3]).

If one of the phases is water, the contact angle is usually, by convention, defined through this phase (i.e. phase 2 in Fig. 1A is water). Depending on the respective interfacial energies, α_2 can be below 30 degrees (hydrophilic particle), between 30 and 90 degrees (partially hydrophobic particle), and above 90 degrees (hydrophobic particle). The energy for transfer of a spherical particle from the bulk of phase 2 to its equilibrium position on the interface is given by the expression [4]

$$U_A = \pi R_P^2 \sigma_{23}(1 + \cos\alpha_2)^2 \tag{2}$$

where R_P is the particle radius. For nanometer and micrometer sized particles, U_A usually exceeds the thermal energy $k_B T$ by many orders of magnitude, unless the contact angle is very small, $\alpha_2 \to 0$.

The term liquid film refers to a liquid phase, which is restricted in one dimension - see Figure 1B. Four types of liquid films, depending on the contacting phases, are usually distinguished [5]: (1) foam films, gas-liquid-gas, (2) emulsion films, liquid-liquid-liquid, (3) suspension films, solid-liquid-solid, and (4) wetting films, solid-liquid-gas or liquid-liquid-gas. The latter are termed also "pseudo-emulsion films" in the literature. The liquid films are often considered as thin or thick, in relation to some characteristic scale. The meaning of these terms, however, can be different in the various research problems. From the viewpoint of liquid film thermodynamics, thin is a film whose thickness is comparable to the range of surface forces (van der Waals, electrostaic, etc.) acting between the two film surfaces. The complete thermodynamic description of such thin films requires one to take into account the surface forces, e.g., via the disjoining pressure [6-9]. Thick is a film, for which the interaction between the two opposing film surfaces can be neglected (typically, for $h > 100$ nm). In hydrodynamic problems, the film is usually called "thin" when its thickness is much smaller than the film radius ($h << R_F$) and one can use the so-called "lubrication approximation" [10, 11]. Note that even films of millimeter thickness can be considered as "thin" according to this definition. A third definition is used in the consideration of films containing solid or fluid particles - the film is thin if the particle size is comparable to (or larger than) the film thickness and vice versa.

2. DYNAMICS OF PARTICLES ON FLUID INTERFACES.

2.1. Determination of the Surface Shear Viscosity and Yield Stress of Adsorption Layers and Lipid Vesicles.

The presence of adsorbed surfactant or polymer molecules on fluid interfaces leads to detectable rheological properties of the interface, such as shear and dilatational viscosity and elasticity [10]. The rheological behavior of the fluid interface is found to play a significant role in various technological processes like formation and transportation of emulsions and foams,

film coating, spraying, ore flotation, oil recovery, etc. [10]. This role is particularly important in foams and emulsions [10-14], where the surface to volume ratio is very high and the interfacial layers can be rather viscous (e.g., in protein stabilized systems). That is why, numerous experimental methods have been suggested in the literature for determination of the surface viscosity [10, 15-24]. Most of these methods, however, are of low sensitivity and only one of them (rotating knife-edge viscometer) can be applied to adsorption layers of soluble low molecular mass surfactants [22-24].

The motion of a particle, which is attached to a fluid interface, is affected by the presence of adsorbed molecules, due to the increased viscous friction in the adsorption layer [25]. Therefore, one way to retrieve information about the interfacial rheological properties is to study the motion of attached particles, under the action of well-defined external force. This idea was utilized in refs. [25, 26], where the drag coefficient of a small spherical particle, attached to air-water interface (bare or covered with surfactant monolayer), was measured. The particle was set in motion under the action of a lateral capillary force, F_L, which is created by a vertical solid wall, used to deform the fluid interface under a controlled manner - see Fig. 2A. The interfacial deformation leads to capillary attraction or repulsion between the particle and the wall, depending on the shape of the meniscus and on the particle mass density [9, 27, 28]. The physical background of the capillary forces and the detailed derivations of the respective formulae are presented in refs [9, 27-29]. For this particular problem, one can use an asymptotic expression [27, 28]

$$F_L = -\pi\sigma\left[2r_C \sin\psi_C \, qHe^{-qx} + q^3 r_C^2 H^2 e^{-2qx}\right]; \qquad xq \gg 1 \qquad (3)$$

which is valid for large particle-wall separation, x, as compared to the capillary length, $1/q$, which characterizes the range of the capillary interaction and is defined as

$$q^{-1} = \left(\sigma / \Delta\rho \, g\right)^{1/2} \qquad\qquad \Delta\rho = \rho_I - \rho_{II} \qquad (4)$$

σ is the tension of the fluid interface, ρ_I and ρ_{II} are the mass densities of the lower and upper fluid phases, and g is the gravity acceleration. In equation (3), H characterizes the

deformation of the interface (see Fig. 2A), r_C is the radius of the three-phase contact line on the particle surface and ψ_C is the angle, characterizing the meniscus slope around the particle-fluid interface contact line (ψ_C can be calculated from the particle mass density and the contact angle α_2, as explained in ref. [28]).

The drag coefficient of the particle was determined by comparing the measured particle trajectory, $x(t)$, with the numerically calculated one by solving the equation of motion

$$m\ddot{x} = F_L - f_d \beta_s \dot{x} \qquad (5)$$

In Eq. (5), $\ddot{x}$ and $\dot{x}$ are the particle acceleration and velocity, respectively, F_L is the lateral capillary force calculated by Eq. (3), and m is the particle mass. The dimensionless particle drag coefficient, f_d, (equal to the actual drag coefficient of the particle, β, normalized by the Stokes coefficient, $\beta_s = 6\pi\eta R_P$) was obtained as an adjustable parameter from the numerical fit to the experimental data. To test the method, the authors investigated [25] the dependence of the particle drag coefficient on the three-phase contact angle for pure air-water interface (negligible interfacial viscosity and elasticity). In this case, theoretical values for f_d are available from the hydrodynamic model developed in ref. [30]. A comparison between the experimentally determined values of f_d and the theoretical predictions, is presented in Fig. 2B for three different values of the particle contact angle. One sees that the agreement between the experimental points and the theoretical curve is very good, with no adjustable parameters being used in the theoretical calculations.

The same experimental procedure was applied to measure the surface shear viscosity of adsorbed surfactant monolayers [26]. In this case, the measured drag coefficient of the particles is larger, due to the viscous friction in the adsorption layer (compare the slopes of the lines shown in Fig. 2C). From the values of f_d one can calculate the surface shear viscosity by using the hydrodynamic model from ref. [30]. The method was applied to three types of surfactants (anionic, cationic, and nonionic) - the surface viscosity of their micellar solutions was determined, see the results shown in Fig. 2C. Note that the method is extremely sensitive

and can be applied to layers of low molecular mass surfactants, which exhibit surface viscosity less than 10^{-6} Pa.m.s - such low values are undetectable by most of the other methods.

The same experimental set-up (Fig. 2A) was used recently [31] to characterize the elastic properties of protein layers of β-lactoglobulin, adsorbed on air-water interface. The lateral particle displacement (in the plane of the adsorption layer) was observed, as a result of oscillatory vertical motion of the barrier with gradually increasing amplitude, H_{MAX}. If the layer behaves as a purely elastic two-dimensional membrane, the particle returns to its initial position at the end of each oscillation of the barrier. However, when the lateral capillary force, F_L, exceeds a certain threshold value, an irreversible displacement of the particle is observed. Thus one can register the threshold capillary force, at which the particle overcomes the restoring elastic force of the protein layer, and to estimate the respective yield stress by using an appropriate model. Since very small lateral capillary forces can be exerted on the particle, it is possible to probe very low values of the yield stress. The data reported in ref. [31] were in a very good agreement with results obtained by other authors with different methods [32, 33].

2.2. Particle Dynamics in Lipid Membranes - Probing the Membrane Viscoelastic Properties.

The shear viscosity of bio-membranes, η_S, is believed to play an important role in the lateral motion of membrane inclusions [34] and in dynamics of cell deformation [35]. The lipid bilayers are considered to be the simplest model of bio-membranes. Most of the literature data on shear viscosity of lipid membranes are obtained by fluorescence techniques [34], which allow one to measure the diffusion coefficient, D_{mol}, of molecular probes embedded in the membrane. The probe is usually modeled as a disk moving inside a continuous layer [36] and η_S is calculated from D_{mol} on the basis of theoretical models. A conceptual difficulty in this approach is created by the fact that the probes are of molecular size, whereas the theoretical models consider them as macroscopic bodies moving in a two-dimensional continuum.

A new method, called "falling ball viscometry" was recently suggested, in which the dynamics of a micro-particle, attached to a lipid bilayer, was studied and interpreted in terms of the membrane rheological properties [37-41]. The experiment is performed with "giant" unilamelar vesicles, obtained by the electroformation method [42, 43] in an optical cuvette. A

latex or glass sphere of diameter in the range between 0.5 and 10 μm is put in contact with the vesicle wall by using a long-working-distance laser optical trap [44]. The experiments show [43] that the latex particle adheres to the vesicle wall and acquires an equilibrium position with a finite contact angle α (Fig. 3). Afterwards, the laser optical trap is switched off, the particle starts moving along the vesicle surface under the action of gravity and Brownian forces, and the particle trajectory is monitored by a microscope connected to a video-camera (cf. Fig. 3B). To interpret adequately the experimental data, the authors developed a complex hydrodynamic model [41], which accounts for the effect of the finite size of the vesicle on the circulation of the internal fluid. For glass spheres of micrometer size, the Peclet number, $Pe = \tilde{m} g \tilde{R} / k_B T$, which is a criterion about the importance of the gravity force as compared to the stochastic Brownian force, is greater than 50, and the particle motion is described by the non-stochastic equation [37]

$$\tilde{m} g \sin\theta = \zeta \, \tilde{R} \frac{d\theta}{dt} \tag{6}$$

where $\tilde{m} g$ is the particle weight corrected for buoyancy, θ is the polar angle defined in Fig. 3A, t is time, and $\tilde{R}$ is the distance between the vesicle and particle centers. For small particles ($Pe < 50$) the particle drag coefficient is more precisely determined from the particle translational diffusion coefficient, D, through the Einstein-Stokes relation, $D = k_B T / \zeta$. The diffusion coefficient in the limit of short times, $\Delta t \to 0$, is determined from the equation (cf. Fig. 3B) [38]

$$\left\langle (\Delta\theta)^2 \right\rangle = \left\langle [(\sin\theta)\Delta\varphi]^2 \right\rangle = \frac{2D}{\tilde{R}^2} \Delta t \tag{7}$$

By using the hydrodynamic model from ref. [41], the authors determined the intrinsic surface shear viscosity of the fluid lipid bilayer from the measured drag coefficients of the particles [44]. The comparison with data of other authors [35], showed a relatively good agreement.

2.3. Ensembles of Particles at Air-Water and Oil-Water Interfaces.

In the following several sections we describe results obtained with ensembles of particles, where the interactions between the particles play a crucial role for the structure and dynamics of the system.

One of the most interesting and beautiful applications of dense 2D particle arrays for simulation of the dynamics of complex atomic systems was described more than 50 years ago [45]. By blowing a large number of monodisperse millimeter-sized bubbles, Sir Lawrence Bragg and J. Nye formed dense mono- and multilayers on the surface of a soap solution. The formed bubble arrays exhibited the main structural characteristics of the metals, such as grain boundaries, dislocations, and disclinations. The structural transformations during various dynamic processes (annealing, re-crystallization, motion of dislocations, shear motion, compression) were observed and analyzed with respect to the metal structure. Following this line, many researchers have used this "analogue model" for studying the structure and dynamics of close-packed 2D crystals [46, 47].

In other studies, dense particle monolayers were studied for probing the lateral interactions between colloid particles attached to an air-water or oil-water interface [48-50]. The layers were compressed in Langmuir trough, the lateral surface pressure was measured as a function of the interparticle spacing and interpreted in terms of the interparticle forces. An interesting conclusion from these studies is that the 2D collapse pressure for particle monolayers is equal to the surface tension of the liquid (both for clean surface and in the presence of surfactant) - an experimental fact, which is explained by the microscopically observed "buckling" mechanism of collapse [50].

A useful information about the general mechanism of particle aggregation in colloid systems could be obtained by direct optical observation of the aggregation process in two dimensions [51-54]. For this purpose, a loose layer of particles is formed on an air-water or oil-water interface, and the dynamics of the particle assembly is observed and analyzed with respect to the particle-particle interactions and aggregate structure. Thus Onoda [51] observed the dynamics of reversible cluster formation of latex particles, floating on air-water interface. The particle diameter was varied between 1 and 15 μm. The author found that the rate of the clustering process and the degree of ordering depended significantly on the particle diameter.

The clusters from small particles were typically well ordered. Furthermore, these clusters were in dynamic equilibrium with a "vapor" of single particles. On the contrary, the clusters obtained from large particles tended to be dendritic (fractal) in shape, because the cluster rearrangement was extremely slow after the particles joined. Taking into account the van der Waals, electrostatic and capillary interactions, the author estimated, that the particle-particle interaction energy varied from 0.2 k_BT (for 1 μm particle) to 10 k_BT (for 10 μm particle), with best order observed for 2 μm particles when the pair interaction energy was around 1 k_BT.

A series of experimental studies, in which the aggregation of modified glass beads (30-75 μm in diameter) at the air-water or octane-water interface, was published by Hórvölgyi and co-workers [52-54]. The growing fractal structures were characterized by particle density functions, which show how the particle number density changes with the aggregate size. The authors estimated the interaction energies between the adsorbed particles, taking into account the van der Waals, electrostatic, hydrophobic and capillary interactions. By varying the ionic strength of the sub-phase, the authors were able to control the particle interactions and the regime of aggregation. They found that at low electrolyte concentration, when restructuring of the already formed aggregates is possible, the fractal dimension of the aggregates depends on the aggregate size and on the experimental conditions (particle hydrophobicity and electrolyte concentration). If, however, the electrolyte concentration was above a certain value, so that the electrostatic repulsion between the particles is suppressed and the restructuring of the aggregates became impossible, the fractal dimension was independent of the particle hydophobicity and on the ionic strength [54].

The role of the particle-particle interactions on the aggregation process was theoretically studied in a series of papers by Meakin [55-58]. He showed that the so called diffusion limited cluster-cluster aggregation model is most realistic among the basic models suggested for description of the aggregation in colloid systems. However, Meakin showed the computer model should be extended to include a variety of processes, which are observed in the real systems, such as reversible attachment/detachment of the particles [55], rotation of the clusters around a point of single contact with another cluster [57], random breaking of bonds in the clusters [56], etc. In general, the combination of computer simulations with experiments on actual colloid systems was very fruitful in revealing the general characteristics of the aggregation processes [58].

3. DYNAMICS OF PARTICLES IN THIN LIQUID FILMS

3.1. Phase Transitions in Two-Dimensional (2D) Colloid Systems.

The basic experimental technique used for observation of 2D phase transitions is schematically shown in Fig. 4A [59-63]. A thin liquid layer, containing monodisperse particles, is formed between two rigid walls, which are slightly inclined toward each other, so that the thickness of the formed slit, h, gradually changes. The suspension in the slit is set in contact with a large reservoir containing a 3D colloid crystal. The particles in the slit are observed by an optical microscope through the transparent glass walls. After allowing the system to equilibrate, which might take days, one can investigate how the particle arrangement in the narrow slit depends on the local film thickness, h, particle concentration, C_{PB}, and ionic strength. The particle trajectories can be tracked and analyzed by a specialized computer software, so that a number of quantitative characteristics, such as various space and space-time correlation functions, mean-square displacements, and others, can be extracted. In some studies [60], the imaging techniques were combined with light diffraction, which allowed the experimentalists to explore both the long-range crystal symmetry and the short-range particle structuring.

The experiments showed [59-62] that the equilibrium particle structures in narrow slits follow a general sequence, which is schematically presented in Fig. 4B. In the thinnest region, where h is smaller than the particle diameter, no particles are found. In the neighboring region with thickness slightly larger than the particle diameter, the spheres arrange in a monolayer possessing a triangular order, denoted by 1Δ. The next, thicker region contains two layers of particles placed one over the other with each of the layers exhibiting a square in-plane order (2□), followed by a bilayer of triangular order (2Δ), etc. The overall sequence of phases, observed in such experiments, is $0 \rightarrow 1\Delta \rightarrow 2\square \rightarrow 2\Delta \rightarrow 3\square \rightarrow ... \rightarrow n\Delta \rightarrow (n+1)\square \rightarrow (n+1)\Delta \rightarrow...$, where n can be as large as 10. At larger h, the particle layers retain a triangular in-plane order, which corresponds to the structure of the bulk 3D colloid crystal in the reservoir. Pieranski et al. [59] showed that such an alternating sequence of triangular and square structures can be explained (at least qualitatively) by a purely geometrical

consideration of the most efficient filling of the available space by the particles. A more detailed theoretical analysis of the above phase-transition sequence requires an explicit consideration of the particle-particle and particle-wall interactions [62]. At moderate and low ionic strengths, often used in these experiments, the prevailing interactions are the hard-core repulsion and the electrostatic interactions. The latter may include a contribution from the image charges, created by the solid walls. Interestingly, the entire range of systems, from highly concentrated hard spheres to one-component plasma (point charges with screened electrostatic interactions), undergo almost the same series of 2D phase transitions [62]. The main difference is that at very low ionic strengths, when a 3D colloid crystal can be formed in the bulk suspension even at low particle concentration (due to the long-ranged, soft electrostatic repulsion), the thin 2D layers remain fluid, i.e. there is no 2D crystalline order.

The above experiments were further extended to investigate in more detail the melting-freezing transition in two dimensions. Murray and co-workers [61, 62] showed that there is a qualitative difference between the topological changes which accompany the melting process in 2D and 3D colloid systems. A relatively sharp interface is observed between the disordered and ordered regions in 3D systems. This interface separates a fluid phase, in which the particles undergo translation diffusion, from a 3D colloid crystal, in which the particles fluctuate around their equilibrium positions in the crystal lattice. The 3D phase transition has all the characteristics of a first-order transition. On the contrary, no distinct boundary can be discerned in melting 2D systems. The decrease of particle concentration, at all remaining parameters fixed, leads to a gradual increase of the number and size of topological defects (disclinations and dislocations) in the crystal lattice until the long-range order is lost. One interesting feature of this transition is that the system passes through an intermediate phase, in which the translation order is disturbed, whereas the long-range orientation order is still preserved. This orientationally ordered fluid is called a hexatic phase and the transition from 2D crystal to a hexatic phase is a second-order phase transition [61, 62]. The further decrease of particle concentration leads to another second-order phase transition from a hexatic phase to a disordered isotropic fluid. Such type of system evolution, comprising a two-stage melting mechanism, and the presence of an intermediate, hexatic phase was predicted by the so called KTHNY theory (under the initials of its authors Kosterlitz, Thouless, Halperin, Nelson, Young, see e.g. ref. [64]) and was directly observed with 2D colloid systems [61, 62].

However, the structure of the actual topological defects observed in the experiments was more complex than the one predicted by the KTHNY theory [64].

The same set-up was used to study the dynamics of crystallization of a 2D colloid layers [62]. One particular feature of the crystallization dynamics in these systems is that the rates of the processes are many orders of magnitude slower than those in atomic systems, which allows one to observe *in situ* the formation of the crystal nuclei, the advance of the crystallization front, and the sequence of structural transformations. In ref. [62], pre-formed 2D crystals were first melted by shearing to a super-cooled liquid, and the process of re-crystallization was observed. The experiments showed that the re-crystallization process typically consisted of several stages. For example, the re-crystallization of a 2□ crystal appears as a sequence of two transitions: (1) from liquid to a buckled 1Δ monolayer, which appears as a quasi-equilibrium intermediate phase, and (2) from 1Δ monolayer to the final equilibrium 2□ crystal. The 1Δ monolayer, formed during the first stage, undergoes domain coarsening and grain boundary annealing until a high degree of crystalline order is achieved. The second stage, which presents a solid-to-solid phase transition, occurs via local rearrangements of the particle positions without a long-distance transfer of particles (so called "martensitic transitions").

One should note that the systems discussed above have some properties, which make them different from other 2D systems, which are encountered in the solid state physics or are simulated in computer experiments. The presence of a suspending fluid, which affects the process dynamics by viscous friction, makes the system rather different from, e.g., the 2D arrays of atoms adsorbed on solid surfaces. Thus the particle energy and momentum are not conserved locally, due to the particle-fluid interaction. Therefore, the conclusions based on experiments with 2D colloid systems should be transferred with care toward atomic and electron systems, especially when the dynamics of the processes is concerned.

3.2. Deposition of Thin Particulate Films on Solid Substrates (Mechanism of Paint Coating and Fabrication of Ordered 2D Arrays).

The research interest to this topic was initially driven by the necessity for a deeper understanding of the mechanisms of painting and paper coating [65, 66]. When a latex

dispersion is spread on a hydrophilic solid substrate and allowed to dry, a continuous, homogeneous film is finally formed. This process of film formation consists of three basic stages: (1) evaporation of water and particle ordering, (2) particle deformation, (3) interdiffusion of polymer across the particle-particle contact zones so that a process of particle fusion (coalescence) takes place [65-67]. We will briefly consider the first stage in water based dispersions, which is closely related to the subject of this paper.

The first models of the process of water evaporation from suspension layers implied a more or less uniform reduction of the layer thickness throughout the surface, until a compact (often ordered) multilayer of particles is formed [67-69]. The van der Waals and electrostatic forces were considered to be of primary importance for the particle arrangement and various theoretical models were suggested to describe the experimentally measured variation of the rate of water evaporation from the evolving layers [68, 69]. Recent optical observations and other experiments showed, however, that the drying process is much more complex than initially thought [65, 66, 70-76]. The experiments showed that most latex dispersions dry with fronts moving along the plane of the substrate, which separate dry from wet regions - see Fig. 5. As the layer dries, the wet zones shrink and the particle packing in the final dry layer is determined mostly by the processes occurring in the transition zone, where the particle concentration corresponds just to the limit of particle immobilization.

Model experiments under well defined conditions [70, 71] showed that the processes occurring in the transition zone are governed mainly by capillary meniscus forces and by a hydrodynamic drag force (Fig. 6). The hydrodynamic drag force appears as a result of water evaporation and it plays an important role for the large-scale transport of the various dispersion components (particles, electrolytes, surfactants). The capillary forces are important in the final stage of the drying process, when the thickness of the aqueous layer becomes smaller than the thickness of the compact particle layer and water-air menisci are formed in the particle array. Two types of capillary forces are distinguished: (1) capillary bridges, which compress the particles against each other, and against the substrate [77], (2) lateral capillary forces, which act in the plane of the substrate facilitating in this way the formation of well ordered, uniform in thickness particle layers [9, 29, 70, 78, 79], see Figure 6. The capillary forces facilitate the formation of the final continuous latex film by causing particle deformation before the complete evaporation of water [65, 66, 80]. The concept of the lateral

drying of coating layers (in the plane of layer) was essential to explain the role of various factors for the drying process, such as the electrolyte and surfactant concentrations, and the shape of the layer surface [65, 66].

The same type of forces (hydrodynamic drag force and capillary forces) provide the possibility for a controlled fabrication of highly ordered mono- and multilayers of particles, which have the potential to be used in several interesting high-tech applications. The experiments showed that under appropriate control of the water evaporation rate and of the meniscus shape, one can obtain a relatively large arrays of well ordered particles [70, 71, 81, 82]. The thickness of the layers can be controlled and can vary from one to ca. hundred layers [82]. The term "convective assembly" is sometimes used in literature for this procedure of particulate layer formation [9]. Interestingly, when thin multilayers are produced, the same sequence of particles arrangement, as shown in Fig. 4B, is observed [70]. 2D arrays of high quality are obtained at lower evaporation rate, in the absence of electrolytes and surfactants, and when working with highly monodisperse and pure suspensions [70, 81, 82].

The ordered particle arrays have a peculiar optical properties, because the particle size and spacing are comparable to the light wavelength [83-89]. The lattice constant and the refractive index of the particles can be varied in wide ranges, so that the optical properties of the arrays can be finely tuned. That is why, such arrays can find application in optical devices (e.g., as diffraction gratings, filters, switches), as photonic elements, and especially as photonic band-gap crystals (periodic dielectric crystals, in which the photons behave in a manner similar to that of electrons in semiconductors) [85-89].

In other studies, the ordered arrays of particles were used as lytographic masks for deposition of regular arrays of metal dots on silicon or for etching of the silicon surface so that regular patterns are formed [90, 91]. Furthermore, the latex arrays can be used as templates to obtain highly porous, well structured materials of desired properties. In this way, porous structures have been obtained during the last several years from a variety of materials, such as inorganic oxides, polymers, glassy carbon, semiconductors, and metals [92-96]. Thus by using a relatively simple and cheap instrumentation one can obtain highly structured arrays with potential applications in the nano-electronics, photonics, and as catalysts [92, 93].

The combination of the convective asembly method with more sophisticated techniques for pre-treatment (patterning) of the substrate surface, leads to a complex textured

surfaces with a desired size and spacing of the structural elements [97, 98]. This makes the method of convective assembly an interesting alternative to the other methods used for production of well ordered particle arrays, such as sedimentation, filtration, slit filling, electrodeposition and others [95, 99]. The development of new methods for particle assembly and for controlled formation of porous structures is currently one of the most rapidly developing branches of materials science, due to the booming interest to nanotechnologies [95, 99].

3.3. Particle Ordering in Foam and Pseudo-emulsion Films.

The investigations of the mechanism of convective assembly on solid surfaces revealed some shortcomings of these substrates. The most important ones are the substrate roughness (except for a specially prepared surfaces like cleaved mica and silicon) and the high probability for immobilization of the particles, due to irreversible sticking to the substrate, before their incorporation inside the ordered array. That is why, the quality of the solid surface (smoothness, hydrophilicity, chemical homogeneity, etc.) is of crucial importance for obtaining arrays of high quality. These observations created an interest towards using liquid substrates for particle assembly, because they have the advantages that their surfaces are molecularly smooth and tangentially mobile.

The first procedure for particle ordering in aqueous films on liquid substrates was developed by Yoshimura et al. [100], who succeeded to obtain 2D crystals of several proteins and protein complexes by spreading protein solution on ultra-pure mercury surface. The 2D protein crystals, obtained after the complete evaporation of water, were transferred to a solid support for fixation and their structure was investigated by electron microscopy and image analysis [100-103]. Well ordered 2D arrays of latex particles were obtained by using mercury [104] and perfluorocarbon oil (PFC) [105] as a substrate. An interesting advantage of the PFC is its high volatility at room temperature, so that the obtained 2D arrays can be deposited gently over a solid substrate after completing the particle assembly process. The optical observations and a large number of experiments on mercury and PFC [103-105] showed that the particle ordering occurs through the same mechanism of convective assembly (as for solid substrates), which is driven by capillary forces and hydrodynamic drag force [9].

Experiments showed [106-108] that well ordered 2D arrays of particles can be assembled by the same mechanism in foam films. In this case no substrate is needed, and the arrays are formed in the space confined between the two foam film surfaces (Fig. 7A). Such arrays are particularly interesting for structural studies of soft, easily deformable particles like vesicles, viruses, protein assemblies, surfactant micelles [109-112]. The aqueous foam films, containing particles, can be vitrified (viz. the water can be transformed into a glassy solid state), by a rapid plunging into a liquid ethane at -185 °C. The samples obtained in this way can be observed by electron microscope at low temperatures, at which the water evaporation from the film is suppressed (so called "electron cryo-microscopy" [109-112]). A major advantage of the vitrification method is that the soft particles preserve their fine structure and no artefacts are created by drying or by using fixation and staining agents, as it often happens in the conventional procedures of sample preparation for electron microscopy. That is why, the vitrification method has found a wide application for investigation of soft, unstable upon drying objects. Since the contrast of particles imbedded in the vitrified ice is relatively low, the structural analysis of such samples usually includes a computer-aided averaging of the particle images over a large set of particles [109-111]. From this viewpoint, the ordered particle arrays or 2D crystals (when available) present the most suitable objects for image analysis. As an illustration, in Figure 7B we present a micrograph of protein-lipid vesicles, which were first ordered by convective assembly in a foam film, then this film was vitrified and the sample was observed by electron cryo-microscopy [108].

The presence of particles turned out to be one of the major factors determining the stability of foam and emulsion films [113-128]. Two qualitatively different cases are distinguished in the literature: (1) when the particles are dispersed inside the film, and (2) when the particles are adsorbed on the film surfaces. In case (1), the films are formed from dispersions, which contain particles of relatively high concentration, so that more or less ordered particle layers are formed in the film interior [113-124]. A typical example for such systems are the foam and emulsion films formed from moderately concentrated surfactant solutions (typically of several wt. %), where the role of particles is played by the surfactant micelles [113-118, 121-123]. As shown experimentally [113-116, 121, 122] and theoretically [113, 117, 120, 123], the layering of particles inside the liquid films gives rise to an oscillatory force between the film surfaces (see Fig. 8), which can be very strong and long-ranged in

comparison with the other surface forces (van der Waals, electrostatic, etc.). Therefore, the stability of many practical disperse systems is determined by these oscillatory forces. The foam, emulsion, and pseudo-emulsion films containing particles, thin in multiple steps - a process which is called stratification in the literature [113-116].

For dispersions of solid spheres, the oscillatory component of the disjoining pressure (force per unit area of the film) can be estimated by the semi-empirical formula [123]

$$\Pi_{OSC} = \begin{cases} P_{OSM} \cos(2\pi h / d_P) \exp(1 - h / d_P) & ; \quad h > d_P \\ -P_{OSM} & ; \quad 0 < h < d_P \end{cases} \tag{8}$$

where h is the film thickness, d_P is the particle diameter, and P_{OSM} is the osmotic pressure of the suspension, which can be calculated by the Carnahan-Starling formula [129]

$$P_{OSM} = \rho_P \, k_B T \frac{1 + \phi + \phi^2 - \phi^3}{(1 - \phi)^3} \quad ; \quad \rho_P = \frac{6\phi}{\pi d_P^3} \tag{9}$$

Here ρ_P is the particle number density and ϕ is the particle volume fraction. For charged particles, one should replace the actual particle diameter with an effective diameter, which includes the counterion atmosphere, $d_{EFF} = (d_P + 2/\kappa)$; κ^{-1} is the Debye screening length. The estimates show that the oscillatory forces are important for foam and emulsion films when the effective volume fraction of the particles is above ca. 20 % [123, 124]. More rigorous numerical approaches and computer simulations were used to describe precisely the oscillatory forces in various systems [117, 120].

In case (2), partially hydrophobic particles are adsorbed on the surfaces of the liquid film and create a steric barrier, which prevents the film thinning and rupture [125-128, 130]. A classical example for such systems are the so called "Pickering emulsions". When the adsorbed particles are spherical and monodisperse, ordered 2D arrays can be obtained under appropriate conditions [130]. Although the particle adsorption energy can be easily calculated for spheres of given size and contact angle (cf. Eq. 2), still there is no general theory explaining the stability of liquid films in the presence of adsorbed particles. Some simple models can be found in refs. [125, 128].

3.4. Effect of Single Particles on Film Stability - Antifoaming.

The capture of solid particles in liquid films (e.g., from the atmosphere) might create serious problems in various technological processes, because the particles easily stick to solid surfaces and create defects in the final product. The deteriorating effect of air-born dust in the electronics manufacturing is a well known technological problem. In coating, the presence of particle in a drying polymer layer can lead either to local thickening of the layer (if the particle is wetted by the liquid) or to rupture of the layer (if the particle is dewetted) - in both cases the uniformity of the layer thickness is disturbed. One should emphasize that the attachment of particles to solid substrates is strongly facilitated by the presence of wetting liquid layers, due to the action of capillary forces (cf. Fig. 6C, D).

In some industries, however, hydrophobic particles are introduced on purpose to destroy undesirable foam [4, 131-135]. For example, the formation of excessive foam in fermentation reactors, paper mills and washing machines can be a serious problem and appropriate additives, called antifoams, are used to reduce the foam volume to an acceptable level. Most often, the antifoams present micrometer sized solid particles, oil drops, or mixed oil-solid globules [131]. Polydimethylsiloxanes or various hydrocarbons are used as oil phase, whereas hydrophobic silica or waxes (e.g., aluminium-magnesium stearate) are used as solid particles. A strong synergistic effect between oil and solid particles is observed in the mixed oil-solid antifoams - usually, they are much more efficient than either of the individual components taken separately [131]. The mixed oil-solid antifoams (if appropriately chosen) can break within seconds foams that would be otherwise stable for hours [136, 137].

A significant progress in the understanding of the mechanism of foam destruction process by antifoams has been achieved during the last years. The foam destruction by solid particles occurs through the so called "bridging-dewetting" mechanism [131, 138-141], which is illustrated in Fig. 9. According to this scenario, the particle should first contact (make a bridge between) the two opposing film surfaces. The formed three-phase contact lines move along the particle surface in an attempt to achieve a position corresponding to the equilibrium three-phase contact angle. If, however, the latter is larger than 90°, the contact lines meet at the particle equator (i.e., the particle is completely dewetted) and an unstable hole is formed in

the foam film, which rapidly expands and destroys the entire film. This process was directly observed by a high-speed cine-camera in a specially designed model experiment [141]. The bridging-dewetting mechanism implies that only very hydrophobic particles, having a contact angle larger than 90°, are active antifoams [4, 134, 140].

The foam destruction by oil containing antifoams (oil drops and mixed oil-solid globules) is more complex and different scenarios are possible [4, 131-137, 142-147] due to the deformability of the antifoam entities - see Fig. 10. Experiments with antifoams comprising silicone oil and hydrophobic silica [137, 146, 147] showed that the antifoam globules form unstable bridges, which rapidly stretch in radial direction, due to uncompensated capillary pressures at the oil-water and oil-air interfaces, and eventually rupture the foam films (bridging-stretching mechanism). Several studies with various antifoams showed that one of the most important factors for the antifoam activity is the facility of globule entry on the foam film surface [131-133, 135, 143, 148-151]. The repulsive forces (e.g., of electrostatic origin) between the antifoam globules and the foam film surfaces, lead to a barrier which prevents the globule entry, so that the bridge formation becomes impossible. In these systems, the antifoam globules are expelled from the thinning foam films into the neighboring meniscus regions (Gibbs-Plateau borders) and the foam remains stable for a long time, minutes or hours [149]. On the contrary, if the entry barrier is low, the antifoam globules are able easily to bridge the foam film surfaces and to destroy the foam film within seconds [137]. The magnitude of the entry barrier was experimentally determined for several antifoam-surfactant couples, and a very good correlation with the antifoam activity was established [151].

REFERENCES

1.   Adamson, W.; Gast, A. P. *Physical Chemistry of Surfaces*, Sixth Edition; John Wiley & Sons: New York, 1997, Chapter 10, 347-389.

2.   Li, D.; Neumann, A. W. Thermodynamic Status of Contact Angles. In *Applied Surface Thermodynamics*, A. W. Neumann, J. K. Spelt, Eds.; Marcel Dekker: New York, 1996, 109-168.

3.   Li, D.; Neumann, A. W. Wettability and Surface Tension of Particles. In *Applied Surface Thermodynamics*, A. W. Neumann, J. K. Spelt, Eds.; Marcel Dekker: New York, 1996, 509-556.

4.   Aveyard, R.; Clint, J. H. Liquid Droplets and Solid Particles at Surfactant Solution Interfaces. J. Chem. Soc. Faraday Trans. **1995**, 91, 2681-2697.

5.   Ter Minassian-Saraga, L. Thin Films Including Layers: Terminology in Relation to Their Preparation and Characterization. Pure Appl. Chem. **1994**, 66, 1667-1738.

6.   Derjaguin, B.V. *Theory of Stability of Colloids and Thin Liquid Films*, Consultant Bureau: New York, 1989.

7.   Ivanov, I.B. Effect of Surface Mobility on The Dynamic Behavior of Thin Liquid Films. Pure Applied Chemistry **1980**, 52, 1241-1262.

8.   De Fejter J.A. Thermodynamics of Thin Liquid Films. In *Thin Liquid Films: Fundamentals And Applications*, Surfactants Science Series Vol. 29, Ivanov, I.B. Ed.; M.Dekker: New York, 1988, Chapter 1.

9.   Kralchevsky, P. A.; Nagayama, K. *Particles at Fluid Interfaces and Membranes: Attachment of Colloid Particles and Proteins to Interfaces and Formation of Two-Dimensional Arrays,* Studies in Interface Science, Vol. 10; Elsevier: Amsterdam, 2001.

10. Edwards, D.A.; Brenner, H.; Wasan, D.T. *Interfacial Transport Processes and Rheology*, Butterworth-Heinemann: Boston, MA (1991).

11. Ivanov I.B.; Dimitrov, D.S. Thin Film Drainage. In *Thin Liquid Films: Fundamentals And Applications*, Surfactants Science Series Vol. 29, Ivanov, I.B. Ed.; M.Dekker: New York, 1988, Chapter 7.

12. Danov K. D. On The Viscosity of Dilute Emulsions. J. Colloid Interface Sci. **2001** - *in press.*

13. Danov, K.D.; Valkovska, D.S.; Ivanov, I.B. Effect of Surfactants on the Film Drainage. J. Colloid Interface Sci. **2000**, 211, 291-303.

14. Malhotra, A.K.; Wasan, D.T. Interfacial Rheological Properties of Adsorbed Surfactant Films with Applications to Emulsion and Foam Stability. In *Thin Liquid Films: Fundamentals And Applications*, Surfactants Science Series Vol. 29, Ivanov, I.B. Ed.; Marcel Dekker, Inc.: New York, 1988, 829-891.

15. Mannheimer, R.J.; Schetcher, R.S. An Improved Apparatus and Analysis for Surface Rheological Measurements. J. Colloid Interface Sci. **1970**, 32,195-211.

16. Goodrich, F.C.; Chatterjee, A.K. The Theory Of Absolute Surface Shear Viscosity II. The Rotating Disk Problem. J. Colloid Interface Sci. **1970**, 34, 36-42.

17. Shail, R.J.; Gooden, D.K. The Slow Rotation of an Axisymmetric Solid Submerged in a Fluid with a Surfactant Surface Layer—II. The Rotating Solid in a Bounded Fluid. Int. J. Multiphase Flow **1981**, 7, 245-260.

18. Oh, S.G.; Slattery, J.C. Disk and Biconical Interfacial Viscometers. J. Colloid Interface Sci. **1978**, 67, 516-525.

19. Brown, A.G.; Thuman, W.C.; Mcbain, J.W. The Surface Viscosity of Detergent Solutions as a Factor in Foam Stability. J. Colloid Sci. **1953**, 8, 491.

20. Davies, J.T.; Rideal, E.K. *Interfacial Phenomena,* Second Edition; Academic Press: New York, 1963.

21. Goodrich, F.C.; Allen, L.H. The Theory of Absolute Surface Shear Viscosity. J. Colloid Interface Sci. **1972**, 40, 329-336.

22. Goodrich, F.C.; Allen, L.H.; Poskanzer, A. A New Surface Viscometer of High Sensitivity I. Theory. J. Colloid Interface Sci. **1975**, 52, 201-212.

23. Poskanzer, A.; Goodrich, F.C. Surface Viscosity of Sodium Dodecyl Sulfate Solutions with and without Added Dodecanol. J. Phys. Chem. **1975**, 79, 2122-2126.

24. Poskanzer, A., Goodrich, F.C. A New Surface Viscometer of High Sensitivity II. Experiments with Stearic Acid Monolayers. J. Colloid Interface Sci. **1975**, 52, 213-221.

25. Petkov, J.T.; Denkov, N.D.; Danov, K.D.; Velev, O.D.; Aust, R.; Durst, F. Measurement of the Drag Coefficient of Spherical Particle Attached to Fluid Interfaces. J. Colloid Interface Sci. **1995**, 171, 147-154.

26. Petkov, J.T.; Denkov, N.D.; Danov, K.D.; Aust, R.; Durst, F. Precise Method for Measuring the Shear Surface Viscosity of Surfactant Monolayers. Langmuir **1996**, 12, 2650-2655.

27. Kralchevsky, P.A.; Paunov, V.N.; Denkov, N.D.; Nagayama, K. Capillary Image Forces: I. Theory. J. Colloid Interface Sci. **1994**, 167, 47-65.

28. Velev, O.D.; Denkov, N.D.; Paunov, V.N.; Kralchevsky, P.A.; Nagayama, K. Capillary Image Forces: II. Experiment. J. Colloid Interface Sci. **1994**, 167, 66-73.

29. Kralchevsky, P.A.; Nagayama, K. Capillary Interactions Between Particles Bound to Interfaces. Liquid Films and Biomembranes. Adv. Colloid Interface Sci. **2000**, 85, 145-192.

30. Danov, K.D.; Aust, R.; Durst, F.; Lange, U. Influence of the Surface Viscosity on the Hydrodynamic Resistance and Surface Diffusivity of a Large Brownian Particle. J. Colloid Interface Sci. **1995**, 175, 36-45.

31. Petkov, J.T.; Gurkov, T.D.; B.E. Campbell, Measurement of the Yield Stress of Gel-Like Protein Layers on Liquid Surfaces by Means of an Attached Particle. Langmuir **2001** - *submitted*.

32. Boerboom, F.J.G.; De Groot-Mostert, A.E.A.; Prins, A.; Van Vliet, T. Bulk and Surface Rheological Behavior of Aqueous Milk Protein Solutions. A Comparison. Neth. Milk & Dairy J. **1996** 50, 183-198.

33. Benjamins, J.; Van Voorst Vader, F. The Determination of the Surface Shear Properties of Adsorbed Protein Layers. Colloids Surfaces **1992** 65, 161-174.

34. Tocanne, J.F.; Dupou-Cezanne, L.; Lopez, A. Lateral Diffusion of Lipids in Model and Natural Membranes. Prog. Lipid Res. **1994** 33, 203-237 and References therein.

35. Waugh, R.E. Surface Viscosity Measurements from Large Bilayer Vesicle Tether Formation I. Analysis. Biophys. J. **1982**, 38, 19-27; *Ibid.* Surface Viscosity Measurements from Large Bilayer Vesicle Tether Formation II. Experiments. **1982**, 38, 29-37.

36. Saffman, P.G. Browinan Motion in Thin Sheets of Viscous Fluid. J. Fluid Mech. **1976**, 73, 593-602; Hughes, B.D.; Pailthorpe, B.A.; White, L.R. The Translational and Rotational Drag on a Cylinder Moving in a Membrane. J. Fluid Mech. **1981**, 110, 349-372.

37. Velikov, K.P.; Dietrich, C.; Hadjiisky, A.; Danov, K.; Pouligny, B. Motion of a Massive Microsphere Bound to a Spherical Vesicle. Europhys. Lett. **1997**, 40, 405-410.

38. Velikov, K.; Danov, K.; Angelova, M.; Dietrich, C.; Pouligny, B. Motion of a Massive Particle Attached to a Spherical Interface: Statistical Properties of the Particle Path. Colloids Surf., A: Physicochem. Eng. Aspects **1999**, 149, 245-251.

39. Dimova, R.; Dietrich, C.; Hadjiisky, A.; Danov, K.; Pouligny, B. Falling Ball Viscosimetry of Giant Vesicle Membranes: Finite-Size Effects. Europian Phys. J. B **1999**, 12, 589-598.

40. Dimova, R.; Dietrich, C.; Pouligny, B. Motion of Particles Attached to Giant Vesicles: Falling Ball Viscosimetry and Elasticity Measurements on Lipid Membranes. In *Giant Vesicles,* Walde P., Luisi P., Eds.; John Willey & Sons: Ltd., 1999, 221.

41. Danov, K.; Dimova, R.; Pouligny, B. Visocus Drag of a Solid Sphere Straddling a Spherical or Flat Interface. Phys. Fluids **2000**, 12, 2711-2722.

42. Angelova, M.I.; Dimitrov, D.S. Mechanism of Liposome Electroformation. Prog. Colloid. Polym. Sci. **1988**, 76, 59-67.

43. Angelova, M.I.; Soléau, S.; Méléard, P.; Faucon, J.F.; Bothorel, P. Preparation of Giant Vesicles by External AC Electric Fields. Kinetics and Applications. Prog. Colloid Polymer Sci. **1992**, 89, 127-131.

44. Angelova, M.I.; Pouligny, B. Trapping and Levitation of a Dielectric Sphere with Off-Centered Gaussian Beams. I. Experimental. Pure Appl. Opt. A **1993**, 2, 261-267.

45. Bragg, L.; Nye, J. F. A Dynamic Model of a Crystal Structure. Proc. Roy. Soc. London **1947**, A190 474-481.

46. Armstrong, A.J.; Mockler, R.C.; O'Sullivan, W.J. Isothermal-Expansion Melting of Two-Dimensional Colloidal Monolayer on the Surface of Water. J. Phys.: Condens. Matter **1989**, 1, 1707-1730.

47. Shaefer, D.W.; Ackerson, B.J. Melting of Colloidal Crystals. Phys. Rev. Lett. **1975**, 35, 1448-1451.

48. Hórvölgyi, Z.; Németh, S.; Fendler, J.H. Monoparticulate Layers of Silanized Glass Spheres at the Water-Air Interface: Particle-Particle and Particle-Subphase Interactions. Langmuir **1996**, 12, 997-1004.

49. Aveyard, R.; Clint, J.H.; Nees, D.; Paunov, V.N. Compression and Structure of Monolayers of Charged Latex Particles at Air-Water and Octane-Water Interfaces. Langmuir **2000**, 16, 1969-1979.

50. Aveyard, R.; Clint, J.H.; Nees, D.; Quirke, N. Structure and Collapse of Particle Monolayer Under Lateral Pressure at the Octane/Aqueous Surfactant Solution Interface. Langmuir **2000**, 16, 8820-8828.

51. Onoda, G. Y. Direct Observation of Two-Dimensional. Dynamic Clustering and Ordering with Colloids. Phys. Rev. Lett. **1985**, 55, 226-229.

52. Hórvölgyi, Z.; Zrínyi, M. Interfacial Aggregation of Floating Microparticles under the Control of Short-Range Colloid and Very Long-Range Capillary Force. Fractals **1993**, 1, 460-469.

53. Hórvölgyi, Z.; Medveczky, G.; Zrínyi, M. On the Structure of Hydrophobed Particles in the Boundary Layer of Water and Octane Phases. Colloid & Polymer Sci. **1993**, 271, 396-403.

54. Hórvölgyi, Z.; Máté, M.; Zrínyi, M. On the Universal Growth of Two-Dimensional Aggregates of Hydrophobed Glass Beads Formed at the (Aqueous Solution of Electrolyte)-Air Interface. Colloids Surfaces A **1994**, 84, 207-216.

55. Meakin, P.; Deutch, J.M. Fractal Structures from an Evaporation/Condensation Model. J. Chem. Phys. **1985**, 83, 4086-4092.

56. Meakin, P. The Effects of Random Bond Breaking on Diffusion Limited Cluster-Cluster Aggregation. J. Chem. Phys. **1985**, 83, 3645-3649.

57. Meakin, P. The Effects of Reorganization Processes on Two-Dimensional Cluster-Cluster Aggregation. J. Colloid Interface Sci. **1986**, 112, 187-194.

58. Meakin, P. Fractal Aggregates. Adv. Colloids Interface Sci. **1988**, 28, 249-331.

59. Pieranski, P.; Strzelecki, L.; Pansu, B. Thin Colloidal Crystals. Phys. Rev. Lett. **1983**, 50, 900-903.

60. Van Winkle, D. H.; Murray, C. A. Layering Transitions In Colloid Crystals As Observed By Diffraction And Direct-Lattice Imaging, Phys. Rev. A **1986**, 34, 562-573.

61. Murray, C. A.; Van Winkle, D. H. Experimental Observation of Two-Stage Melting in a Classical Two-Dimensional Screened Coulomb System. Phys. Rev. Lett. **1987**, 58, 1200-1203.

62. Murray, C. A.; Grier, D. G. Video Microscopy of Monodisperse Colloidal Systems. Annu. Rev. Phys. Chem. **1996**, 47, 421-462.

63. Skjeltorp, A. T.; Meakin, P. Simulation of Random and Ordered Systems Using Experimental and Numerical Methods. In *Hydrodynamics Of Dispersed Media.* Hulin, J. P.; Cazabat, A. M.; Guyon, E.; Carmona, F., Eds.; Elsevier: Amsterdam, 1990; 139-154.

64. Nelson, D.R. In *Phase Transitions and Critical Phenomena*. Domb, C.; Lebowitz, J.L. Eds.; Academic: London, 1983, 7, 1-99.

65. Keddie, J. L. Film Formation of Latex. Mater. Sci. Engin. **1997**, 21, 101-107.

66. Winnik, M. A. Latex Film Formation. Current Opinion Colloid Interface Sci. **1997**, 2, 192-199.

67. Vanderhoff, J. W.; Bradfod, E. B.; Carrington, W. K. The Transport of Water Through Latex Films. J. Polymer Sci. Symp. **1973**, 41, 155-174.

68. Croll, S. G. Drying of Latex Paint. J. Coating Technol. **1986**, 58, 41-49.

69. Eckersley, S. T.; Rudin, A. Drying Behaviour of Acrylic Latexes. Progress Org. Coating **1994**, 23, 387-402.

70. Denkov, N. D.; Velev, O. D.; Kralchevsky, P. A.; Ivanov, I. B.; Nagayama, K.; Yoshimura, H. Mechanism of Formation of Two-Dimensional Crystals From Latex Particles on Substrates. Langmuir **1992**, 8, 3183-3190.

71. Denkov, N. D.; Velev, O. D.; Kralchevsky, P. A.; Ivanov, I. B.; Nagayama, K.; Yoshimura, H. Two-Dimensional Crystallization. Nature **1993**, 361, 26.

72. Juhie, D.; Lang, J.; Wang, Y.; Leung, O. M.; Goh, M. C.; Winnik, M. A. Surfactant Exudation in the Presence of a Coalescing Aid in Latex Films Studied by Atomic Force Microscopy. J. Polymer Sci. B: Polymer Phys. **1995**, 33, 1123-1133.

73. Winnik, M. A. The Formation and Properties of Latex Films. In *Emulsion Polymerization And Emulsion Polymers,* Lovell, P. A.; El-Aasser, M. S., Eds.; Wiley: New York, 1997, 468-518.

74. Winnik, M. A.; Feng, J. Latex Blends: An Approach to Zero VOC Coatings. J. Coating Technol. **1996**, 68, 39-50.

75. Ming, Y.; Takamura, K.; Davis, H. T.; Scriven, L. E. Microstructure Evolution in Latex Coatings. Tappi J. **1995**, 78, 151-159.

76. Dobler, F.; Holl, Y. Mechanisms of Latex Film Formation. Trend Polymer Sci. **1996**, 4, 272-279.

77. Israelachvili, J.N. *Intermolecular And Surface Forces*. Second Edition; Academic Press: London, 1992, Chapter 15.

78. Velev, O. D.; Denkov, N. D.; Paunov, V. N.; Kralchevsky, P. A.; Nagayama, K. Direct Measurement of Lateral Capillary Forces. Langmuir **1993**, 9, 3702-3709.

79. Dushkin, C. D.; Kralchevsky, P. A.; Yoshimura, H.; Nagayama, K. Lateral Capillary Forces Measured by Torsion Microbalance. Phys. Rev. Lett. **1995**, 75, 3454-3457.

80. Visschers, M.; Laven, J.; German, A. L. Current Understanding of the Deformation of Latex Particles During Film Formation. Progress Org. Coating **1997**, 30, 39-49.

81. Dimitrov, A. S.; Nagayama, K. Continuous Convective Assembling of Fine Particles into Two-Dimensional Arrays on Solid Surfaces. Langmuir **1996**, 12, 1303-1311.

82. Jiang, P.; Bertone, J. F.; Hwang, K. S.; Colvin, V. L. Single Crystal Colloidal Multilayers of Controlled Thickness. Chem. Mater. **1999**, 11, 2132-2140.

83. Hayashi, S.; Kumamoto, Y.; Suzuki, T.; Hirai, T. Imaging by Polystyrene Latex Particles. J. Colloid Interface Sci. **1991**, 144, 538-547.

84. Dushkin, C. D.; Nagayama, K.; Miwa, T.; Kralchevsky, P. A. Colored Multilayers From Transparent Submicrometer Spheres. Langmuir **1993** 9, 3695-3701.

85. Matsushita, S. I.; Yagi, Y.; Miwa, T.; Tryk, D. A.; Koda, T.; Fujishima, A. Light Propagation in Composite Two-Dimensional Arrays of Polystyrene Spherical Particles. Langmuir **2000**, 16, 636-642.

86. Yagi, Y.; Matsushita, S. I.; Tryk, D. A.; Koda, T.; Fujishima, A. Obsrevation of Light Propagation in Single Layers of Composite Two-Dimensional Arrays. Langmuir **2000**, 16, 1180-1184.

87. Zhao, Y.; Auvritsky, I.; Li, B. Optical Coupling Between Monocrystalline Colloidal Crystals and a Planar Waveguide. Appl. Phys. Lett. **1999**, 75, 3596-3598.

88. Park, S. H.; Xia, Y. Assembly of Mesoscale Particles over Large Areas and Its Application in Fabricating Tunable Optical Filters. Langmuir **1999**, 15, 266-273.

89. Ohara, P. C.; Gelbart, W. M. Interplay Between Hole Instability and Nanoparticle Array Formation in Ultrathin Liquid Films. Langmuir **1998**, 14, 3418-3424.

90. Deckman, H. W.; Dunsmuir, J. H. Natural Lithography. Appl. Phys. Lett. **1982**, 41, 377-378.

91. Deckman, H. W.; Dunsmuir, J. H.; Garoff, S.; Mchenry, J. A.; Peiffer, D. G. Macromolecular Self-Organized Assemblies. J. Vac. Sci. Technol. B **1988**, 6, 333-336.

92. Velev, O. D.; Jede, T. A.; Lobo, R. F.; Lenhoff, A. M. Porous Silica Via Colloidal Crystallization. Nature **1997**, 389, 447-448.

93. Velev, O. D.; Jede, T. A.; Lobo, R. F.; Lenhoff, A. M. Microstructured Porous Silica Obtained Via Colloidal Crystal Templates. Chem. Mater. **1998**, 10, 3597-3602.

94. Holland, B. T.; Blanford, C. F.; Stein, A. Synthesis of Macroporous Minerals with Highly Ordered Three-Dimensional Arrays of Spheroidal Voids. Science **1998**, 281, 538-540.

95. Velev, O. D.; Lenhoff, A. M. Colloidal Crystals as Templates for Porous Materials. Curr. Opinion Colloid Interface Sci. **2000**, 5, 56-63.

96. Park, S. H.; Qin, D.; Xia, Y. Crystallyzation of Mesoscale Particles over Large Areas. Adv. Mater. **1998**, 10, 1028-1032.

97. Aizenberg, J.; Braun, P. V.; Wiltzius, P. Patterned Colloidal Deposition Controlled by Electrostatic and Capillary Forces. Phys. Rev. Lett. **2000**, 84, 2997-3000.

98. Qin, D.; Xia, Y.; Xu, B.; Yang, H.; Zhu, C.; Whitesides, G. M. Fabrication of Ordered Two-Dimensional Arrays of Micro- and Nanoparticles Using Patterned Self-Assembled Monolayers as Templates. Adv. Materials **1999**, 11, 1433-1437.

99. Xia, Y.; Rogers, A. J.; Paul, K. E.; Whitesides, G. M. Unconventional Methods for Fabricating and Patterning Nanostructures. Chem. Rev. **1999**, 99, 1823-1848.

100. Yoshimura, H.; Matsumoto, M.; Endo, S.; Nagayama, K. Two-Dimensional Crystallization of Proteins on Mercury. Ultramicroscopy **1990**, 32, 265-274.

101. Akiba, T.; Yoshimura, H.; Namba, K. Monolayer Crystallization of Flagelar L-P Rings by Sequential Addition and Depletion of Lipid. Science **1991**, 252, 1544-1546.

102. Ishii, N.; Taguchi, H.; Yoshida, M.; Yoshimura, H.; Nagayama, K. Image Analysis by Electron Microscopy of Two-Dimensional Crystals Developed on a Mercury Surface of Chaperonin from *Thermus Thermophilus*. J. Biochem. **1991**, 110, 905-908.

103. Nagayama, K. Fabrication of Protein Crystalline Films on Mercury. Mater. Sci. Engin. **1994**, C1, 87-94.

104. Yamaki, M.; Matsubara, K.; Nagayama, K. A Thin Liquid Layer on the Surface of Mercury as a Matrix of a Flow-Mediated Two-Dimensional Assembly of Proteins. Langmuir **1993**, 9, 3154-3158.

105. Lazarov, G. S.; Denkov, N. D.; Velev, O. D.; Kralchevsky, P. A.; Nagayama, K. Formation of Two-Dimensional Structures from Colloid Particles on Fluorinated Oil Substrate. J. Chem. Soc. Faraday Trans. **1994**, 90, 2077-2083.

106. Denkov, N. D.; Yoshimura, H.; Nagayama, K. Nanoparticle Arrays in Freely Suspended Vitrified Films. Phys. Rev. Lett. **1996**, 76, 2354-2357.

107. Denkov, N. D.; Yoshimura, H.; Nagayama, K. Method for Controlled Formation of Vitrified Films for Cryo-Electron Microscopy. Ultramicroscopy **1996**, 65, 147-158.

108. Denkov, N. D.; Yoshimura, H.; Kouyama, T.; Walz, J.; Nagayama, K. Electron Cryomicroscopy of Bacteriorhodopsin Vesicles: Mechanism of Vesicle Formation. Biophys. J. **1998**, 74, 1409-1420.

109. Adrian, M.; Dubochet, J.; Lepault, J.; Mcdowall, A. W. Cryo-Electron Microscopy of Viruses. Nature **1984**, 308, 32-36.

110. Dubochet, J.; Adrian, M.; Chang, J.-J.; Homo, J.-C.; Lepault, J.; Mcdowall, A. W.; Schultz, P. Cryo-Electron Microscopy of Vitrified Specimens. Quart. Rev. Biophys. **1998**, 21, 129-228.

111. Chiu, W. What Does Electron Cryomicroscopy Provide That X-Ray Crystallography and NMR Spectroscopy Cannot? Annu. Rev. Biophys. Biomol. Struct. **1993**, 22, 233-255.

112. Talmon, Y. Transmission Electron Microscopy of Complex Fluids: The State of the Art. Ber. Bunsenges. Phys. Chem. **1996**, 100, 364-372.

113. Nikolov, A.D.; Wasan, D.T.; Kralchevsky, P.A.; Ivanov, I. B.; Ordered Micelle Structuring in Thin Films Formed from Anionic Surfactant Solutions: 1. Experimental. 2. Model Development. J. Colloid Interface Sci. **1989**, 133, 1-12, 13-22.

114. Kralchevsky, P. A.; Nikolov, A. D.; Wasan, D. T.; Ivanov, I. B. Formation and Expansion of Dark Spots in Stratifying Foam Films. Langmuir **1990**, 6, 1180-1189.

115. Wasan, D. T.; Nikolov, A. D.; Kralchevsky, P. A.; Ivanov, I. B. Universality in Film Stratification Due to Colloid Crystal Formation. Colloids Surfaces **1992**, 67, 139-145.

116. Bergeron, V.; Radke, C. J. Equilibrium Measurements of Oscillatory Disjoining Pressures in Aqueous Foam Films. Langmuir **1992**, 8, 3020-3026.

117. Pollard, M. L.; Radke, C. J. Density-Functional Modeling of Structure and Forces in Thin Micellar Liquid Films. J. Chem. Phys. **1994**, 101, 6979-6991.

118. Krichevsky, O.; Stavans, J. Micellar Stratification in Soap Films: A Light Scattering Study. Phys. Rev. Lett. **1995**, 74, 2752-2755.

119. Hug, J. E.; Van Swol, F.; Zukoski, C. F. The Freezing of Colloidal Suspensions in Confined Space. Langmuir **1995**, 11, 111-118.

120. Chu, X. L.; Nikolov, A. D.; Wasan, D. T. Monte Carlo Simulation of Inlayer Structure Formation in Thin Liquid Films. Langmuir **1994**, 10, 4403-4408.

121. Marinova, K. G.; Gurkov, T. D.; Dimitrova, T. D.; Alargova, R. G.; Smith, D. Role of Oscillatory Structural Forces for Interactions in Thin Emulsion Films Containing Micelles. Langmuir **1998**, 14, 2011-2019.

122. Richetti, P.; Kekicheff, P. Direct Measurement of Depletion and Structural Forces in a Micellar System. Phys. Rev. Lett. **1992**, 68, 1951-1954.

123. Kralchevsky, P. A.; Denkov, N. D. Analytical Expression for the Oscillatory Structural Surface Forces. Chem. Phys. Lett. **1995**, 240, 385-392.

124. Kralchevsky, P. A.; Danov, K. D.; Denkov, N. D. Chemical Physics of Colloid Systems and Interfaces. In *Handbook Of Surface And Colloid Chemistry*, K. S. Birdi, Ed.; CRC Press: Boca Raton, FL, 1997, 333-494.

125. Tambe, D.E.; Sharma, M. M. The Effect of Colloidal Particles on Fluid-Fluid Interfacial Properties and Emulsion Stability. Adv. Colloids Interface Sci. **1994**, 52, 1-63.

126. Binks, B. P.; Lumsdon, S. O. Catastrophic Phase Inversion of Water-In-Oil Emulsions Stabilized by Hydrophobic Silica. Langmuir **2000**, 16, 2539-2547.

127. Binks, B.P.; Lumdson, S.O. Influence of Particle Wettability on the Type and Stability of Surfactant-Free Emulsions. Langmuir **2000**, 16, 8622-8631.

128. Denkov N. D.; Kralchevsky, P. A.; Ivanov, I. B.; Wasan, D. T. A Possible Mechanism of Stabilization of Emulsions by Solid Particles. J. Colloid Interface Sci. **1992**, 150, 589-593.

129. Carnahan, N.F.; Starling, K.E. Equation of State for Nonattracting Rigid Spheres. J. Chem. Phys. **1969**, 51, 635-641.

130. Velikov, K. P.; Durst, F.; Velev, O. D. Direct Observation of the Dynamics of Latex Particles Confined Inside Thinning Water-Air Film. Langmuir **1998**, 14, 1148-1155.

131. Garrett, P. R. The Mode of Action of Antifoams. In *Defoaming: Theory And Industrial Applications,* P. R. Garrett, Ed.; Marcel Dekker: New York, 1993, 1-118.

132. Wasan, D. T.; Cristiano, S. P. Foams and Antifoams: A Thin Film Approach. In *Handbook Of Surface And Colloid Chemistry*, K. S. Birdi, Ed.; CRC Press: Boca Raton, FL, 1997; 179-215.

133. Exerowa, D.; Kruglyakov, P. M. *Foam and Foam Films*, Elsevier: Amsterdam, 1998, Chapter 9.

134. Aveyard, R.; Binks, B.P.; Fletcher, P.D.I.; Peck, T.-G.; Rutherford, C.E. Aspects of Aqueous Foam Stability in the Presence of Hydrocarbon Oils and Solid Particles. Adv. Colloid Interface Sci. **1994**, 48, 93-136.

135. Bergeron, V.; Cooper, P.; Fischer, C.; Giermanska-Kahn, J.; Langevin, D.; Pouchelon, A. Polydimethylsiloxane (PDMS)-Based Antifoams. Colloids Surf., A: Physicochem. Eng. Aspects **1997**, 122, 103-120.

136. Koczo, K.; Koczone, J.K.; Wasan, D.T. Mechanisms for Antifoaming Action in Aqueous Systems by Hydrophobic Particles and Insoluble Liquids. J. Colloid Interface Sci. **1994**, 166, 225-238.

137. Denkov, N. D.; Cooper, P.; Martin, J.-Y. Mechanisms of Action of Mixed Solid-Liquid Antifoams: 1. Dynamics of Foam Film Rupture. Langmuir **1999**, 15, 8514-8529.

138. Aronson, M. P.; Influence of Hydrophobic Particles on the Foaming of Aqueous Surfactant Solutions. Langmuir **1986**, 2, 653-659.

139. Frye, G. C.; Berg, J. C. Antifoam Action by Solid Particles. J. Colloid Interface Sci. **1989**, 127, 222-238.

140. Aveyard, R.; Binks, B. P.; Fletcher, P. D. I.; Rutherford, C. E. Contact Angles in Relation to the Effects of Solids on Film and Foam Stability. J. Dispersion Sci. Technol. **1994**, 15, 257-271.

141. Dippenaar, A. The Destabilization of Froth by Solids, 1. The Mechanism of Film Rupture. Int. J. Mineral Process. **1982**, 9, 1-14.

142. Aveyard, R.; Cooper, P.; Fletcher, P. D. I.; Rutherford, C. E. Foam Breakdown by Hydrophobic Particles and Nonpolar Oil. Langmuir **1993**, 9, 604-613.

143. Aveyard, R.; Binks, B. P.; Fletcher, P. D. I.; Peck, T.-G.; Garrett, P. R. Entry and Spreading of Alkane Drops at the Air/Surfactant Solution Interface in Relation to Foam and Soap Film Stability. J. Chem. Soc. Faraday Trans. **1993**, 89, 4313-4321.

144. Garrett, P. R. Preliminary Considerations Concerning the Stability of a Liquid Heterogeneity in a Plane-Parallel Liquid Film. J. Colloid Interface Sci. **1980**, 76, 587-590.

145. Garrett, P. R.; Davis, J., Rendal, H. M. An Experimental Study of the Antifoam Behaviour of Mixtures of a Hydrocarbon Oil and Hydrophoic Particles. Colloids Surfaces A: Physicochem. Engin. Aspects **1994**, 85, 159-197.

146. Denkov, N. D. Mechanisms of Action of Mixed Solid-Liquid Antifoams: 2. Stability of Oil Bridges in Foam Films. Langmuir **1999**, 15, 8530-8542.

147. Denkov, N. D.; Marinova, K.; Hristova, H.; Hadjiiski, A.; Cooper, P. Mechanisms of Action of Mixed Solid-Liquid Antifoams: 3. Exhaustion and Reactivation. Langmuir **2000**, 16, 2515-2528.

148. Kulkarni, R. D.; Goddard, E. D.; Kanner, B. Mechanism of Antifoaming Action. J. Colloid Interface Sci. **1977**, 59, 468-476.

149. Basheva, E. S.; Ganchev, D.; Denkov, N. D.; Kasuga, K.; Satoh, N.; Tsujii, K. Role of Betaine as Foam Booster in the Presence of Silicone Oil Drops. Langmuir **2000**, 16, 1000-1013.

150. Lobo, L.; Wasan, D. T. Mechanisms of Aqueous Foam Stability in the Presence of Emulsified Non-Aqueous-Phase Liquids: Structure and Stability of the Pseudoemulsion Film. Langmuir **1993**, 9, 1668-1677.

151. Hadjiiski, A.; Denkov, N. D.; Tcholakova, S.; Ivanov, I. B. Role of Entry Barriers in the Foam Destruction by Oil Drops. In *Proc. 13th International Symposium on Surfactants in Solutions*, June 2000, Gainsville, Florida – *in press*.
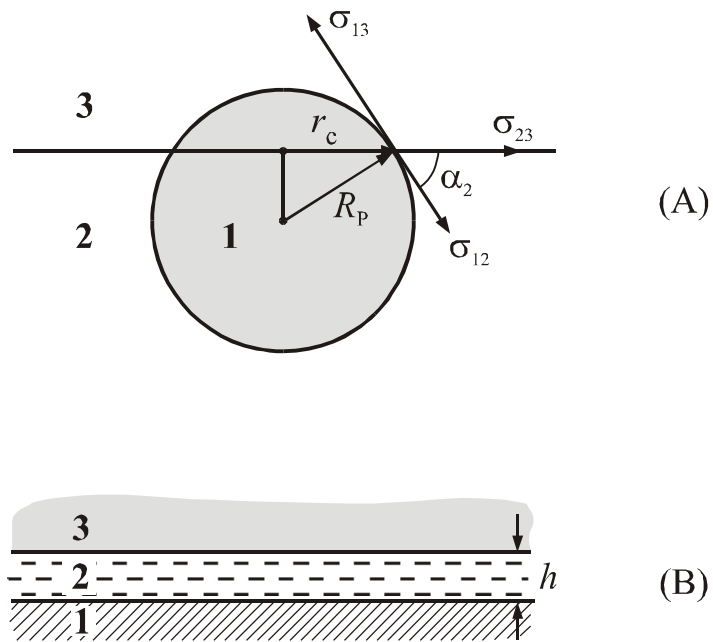
Figure 1. (A) Spherical solid particle (phase 1) attached to the fluid interface between phases 2 and 3; R_P is the particle radius, r_C is the radius of the three-phase contact line, and α_2 is the three--phase contact angle measured through phase 2. (B) A liquid film of phase 2, formed between phases 1 and 3. Depending on the phases one can distinguish: foam films (gas/liquid/gas), emulsion films (liquid-liquid-liquid), suspension films (solid-liquid-solid), and wetting films (solid-liquid-gas or liquid-liquid-gas).
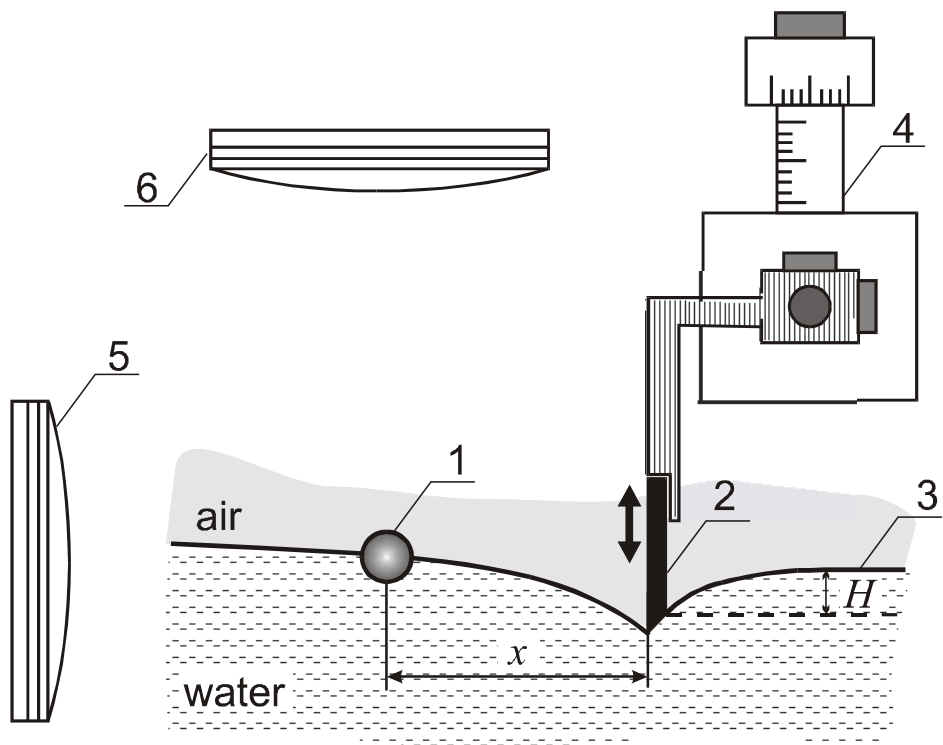
(A)
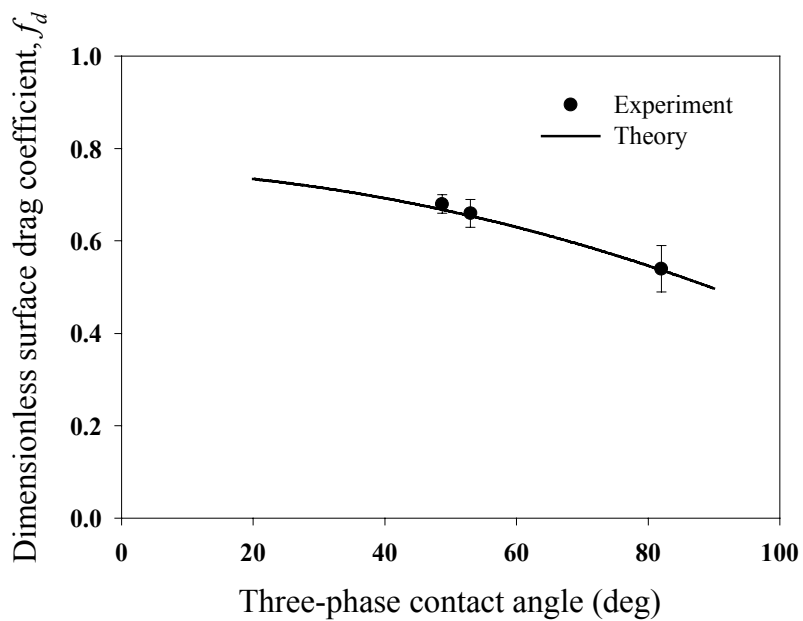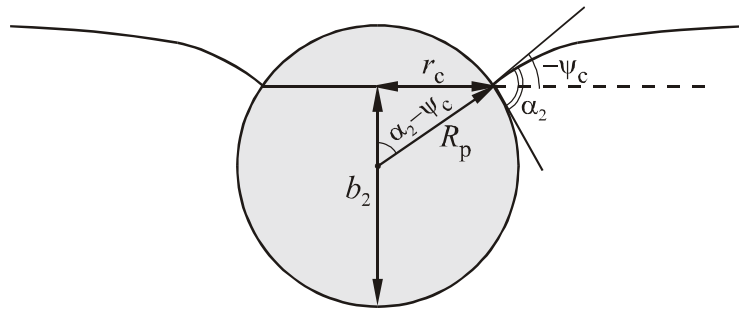
(B)
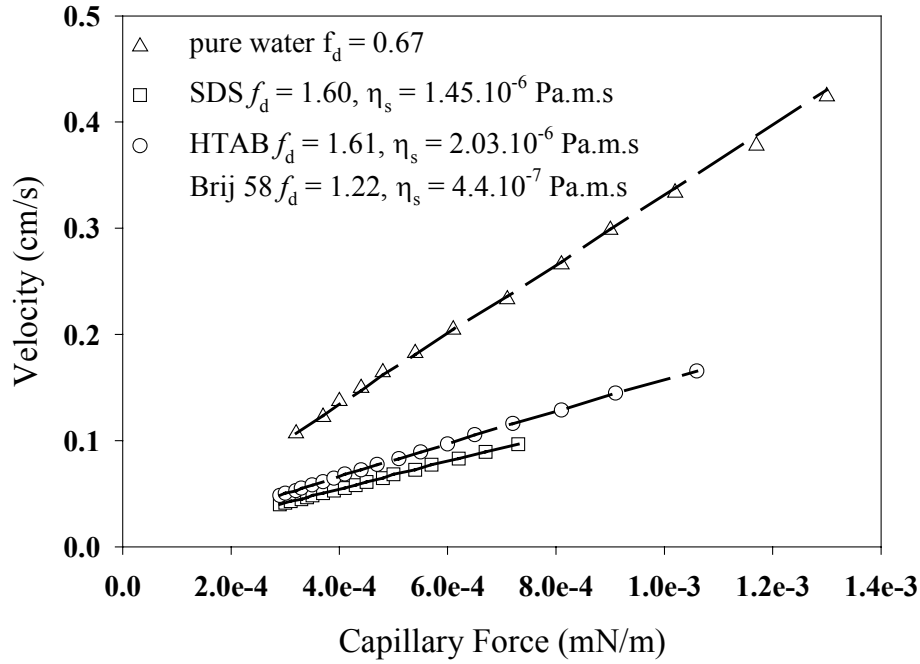
(C)

Figure 2. (A) Schematic presentation of the experimental set-up used in the experiments for determination of the surface viscosity, η_S, from the drag coefficient, f_d, of a "sliding" particle [26]. The particle configuration at the interface is also shown - ψ_2 is the meniscus slope angle at the contact line. (B) Comparison between experimentally determined values of f_d (symbols) and the theoretically calculated solid curve for pure water, according to the model from ref. [30]. (C) Dependence of the particle velocity on the applied capillary force for pure water and for surfactant solutions of sodium dodecyl sulfate (SDS) and hexadecyl trimethyl-ammonium bromide (HTAB). The slopes of the lines are inversely proportional to the dimensionless drag coefficients, f_d, from which the surface viscosity, η_S, can be determined [30].
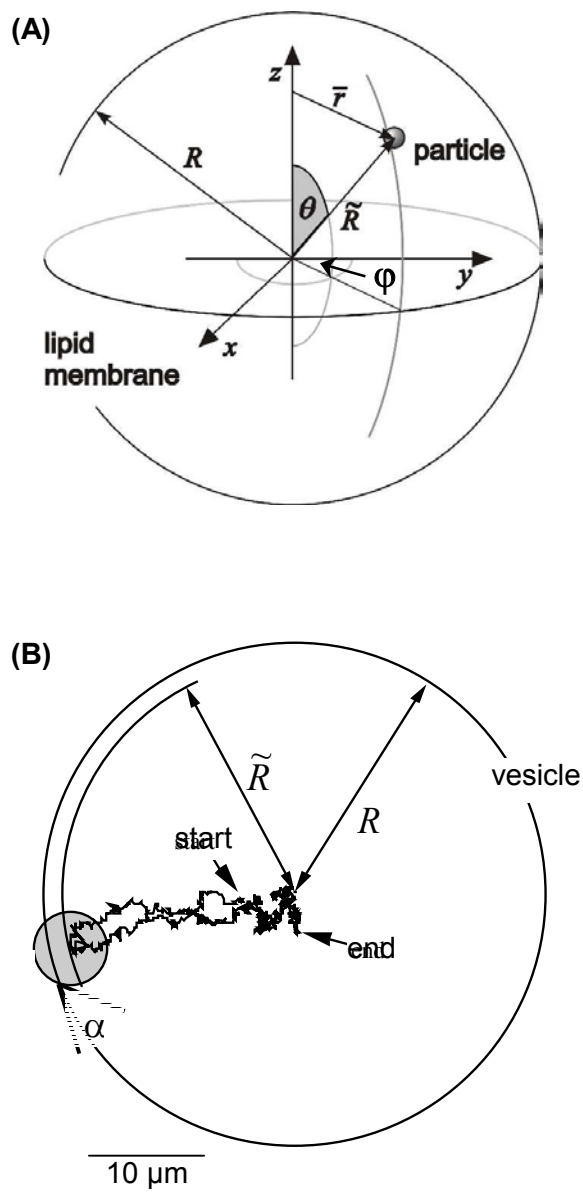
Figure 3. Falling ball viscosimetry of giant lipid vesicles [39]. (A) Schematic presentation of the particle position on the vesicle surface. (B) Particle path on the vesicle surface.
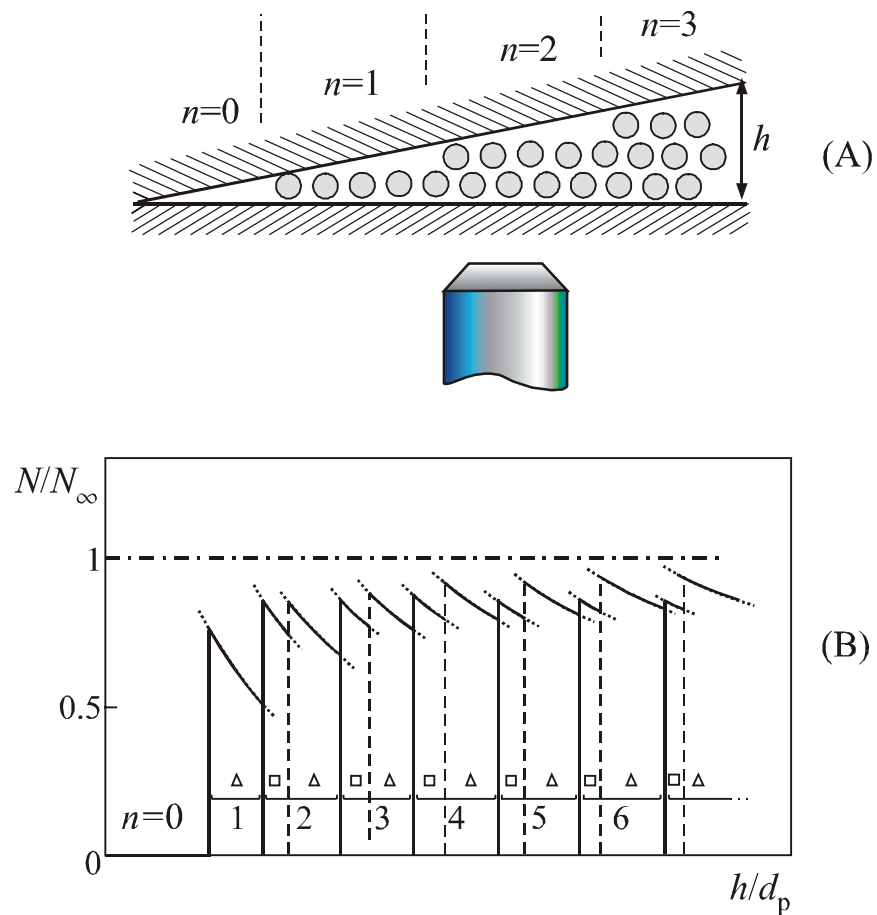
Figure 4. (A) Schematic presentation of the experimental cell for observation of 2D phase transitions in colloid systems: h is the local film thickness and n shows the number of layers. (B) Experimentally observed phase diagram with charged latex particles: the symbols $\triangle$ and $\square$ indicate the type of the observed in-plane lattice; d_P is the particle diameter; and N/N_∞ is the local particle number concentration, normalized by the particle concentration in the bulk suspension (adapted from ref. [59]).
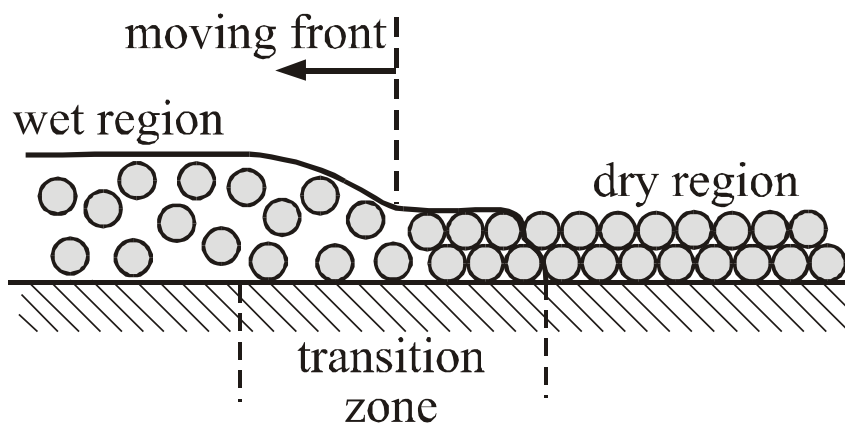
Figure 5. Schematic presentation of the drying process for latex dispersion spread on a solid substrate [65, 66]. The dry and wet regions are separated by a transition zone called also "the compaction front". A flux of water, which drags the suspended particles towards the periphery of the wet region, is caused by water evaporation in the transition zone (see also Fig. 6A,B). As drying proceeds, the dry region increases in size at the expense of the wet region, i.e. the drying front propagates in direction opposite to that of the water flux.
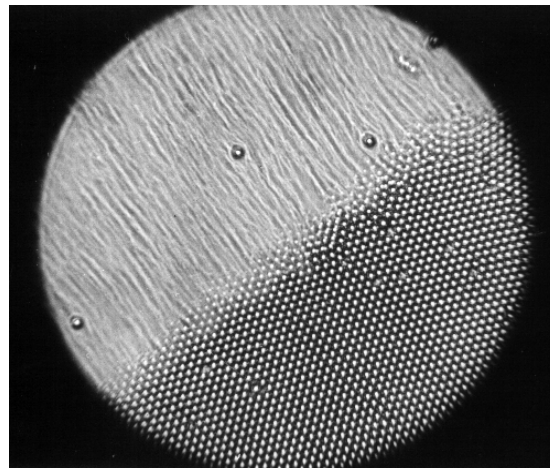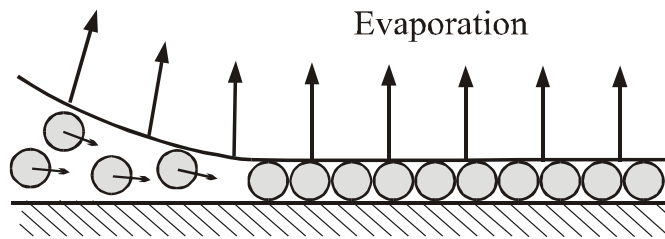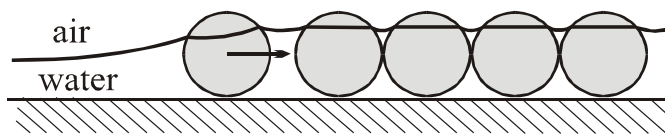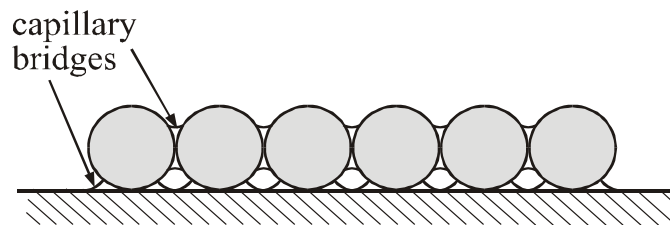
Figure 6. Mechanism of ordering of micro-particles in wetting films [9, 70, 71]. (A) Micrograph of the process of 2D array formation from latex particles of diameter 1.7 μm. The tracks of the particles moving toward an already ordered region are seen in the upper left half of the picture (optical microscopy in transmitted white light). (B) The directed motion of the suspended particles in the disordered region is due to convective water flux, which carries along the particles toward the ordered array. This convective flux is caused by the water evaporation - once the ordered array is formed, the thinning of the aqueous layer in the array is slowed due to the particle hydrophilicity. As a result, the ordered array "soaks" liquid from the neighboring thicker regions to compensate the evaporating water. (C) At a later stage of the drying process, when the thickness of the aqueous layer in the transition region becomes smaller than the particle diameter, a lateral capillary force (indicated by arrow) appears between the particles - for details see refs. [9, 29, 70]. (D) During the final stage of drying, liquid bridges strongly compress the particles against each other and against the substrate [65, 66, 80].
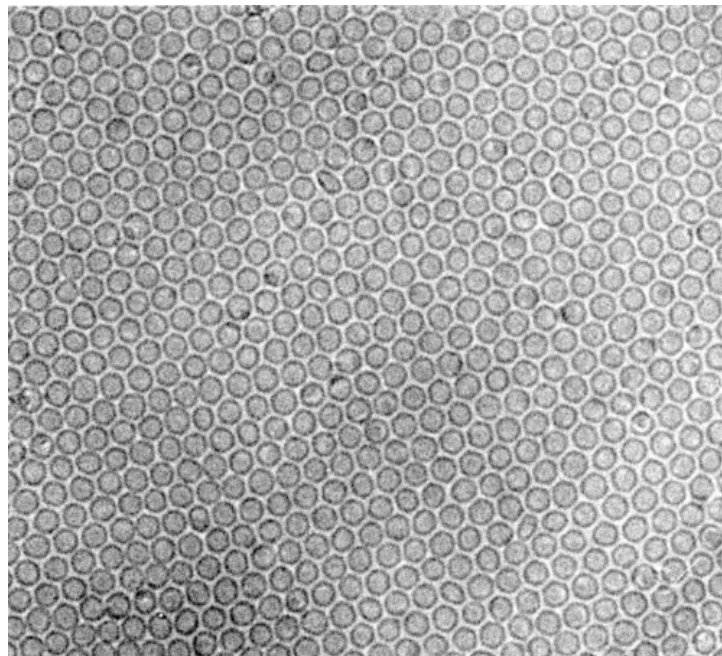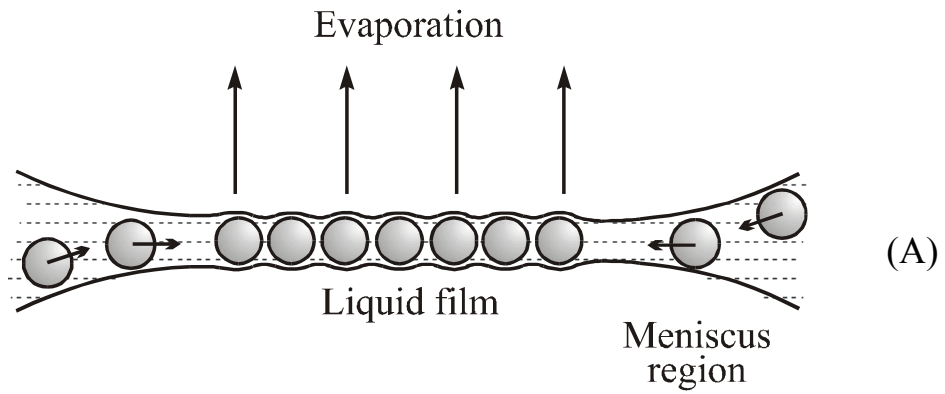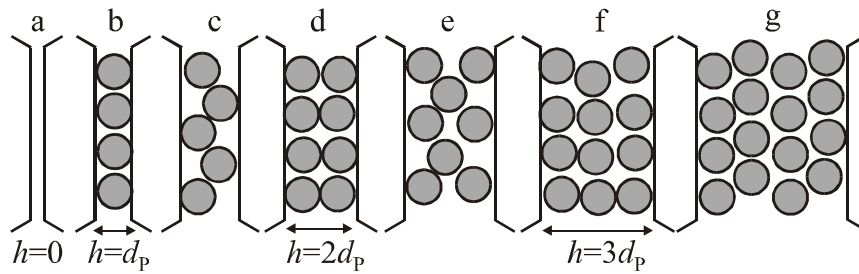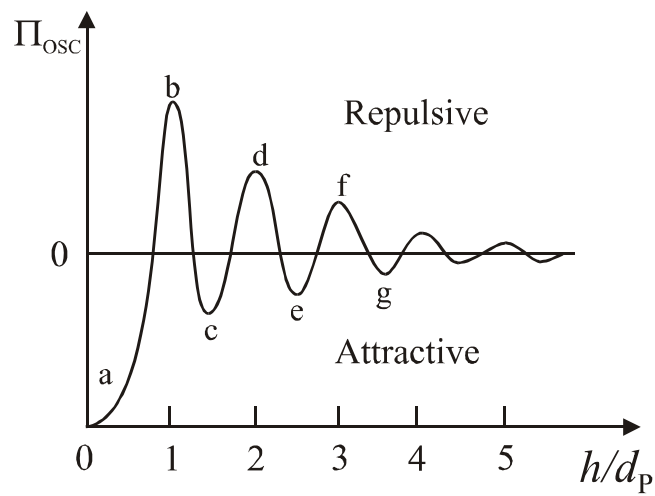
Figure 7. (A) Schematic presentation of the process of convective assembly of mono-disperse particles in foam films [106]. (B) Electron micrograph of an ordered 2D array of lipid-protein vesicles in vitrified foam film [108]. The vesicle diameter is 31 ± 2 nm.

Figure 8. (A) More or less ordered particle layers appear in the liquid films when the film thickness becomes comparable to the particle size. (B) These layers lead to a strong and long-ranged oscillatory contribution to the disjoining pressure (force per unit area), which acts between the film surfaces (adopted from ref. [77]).
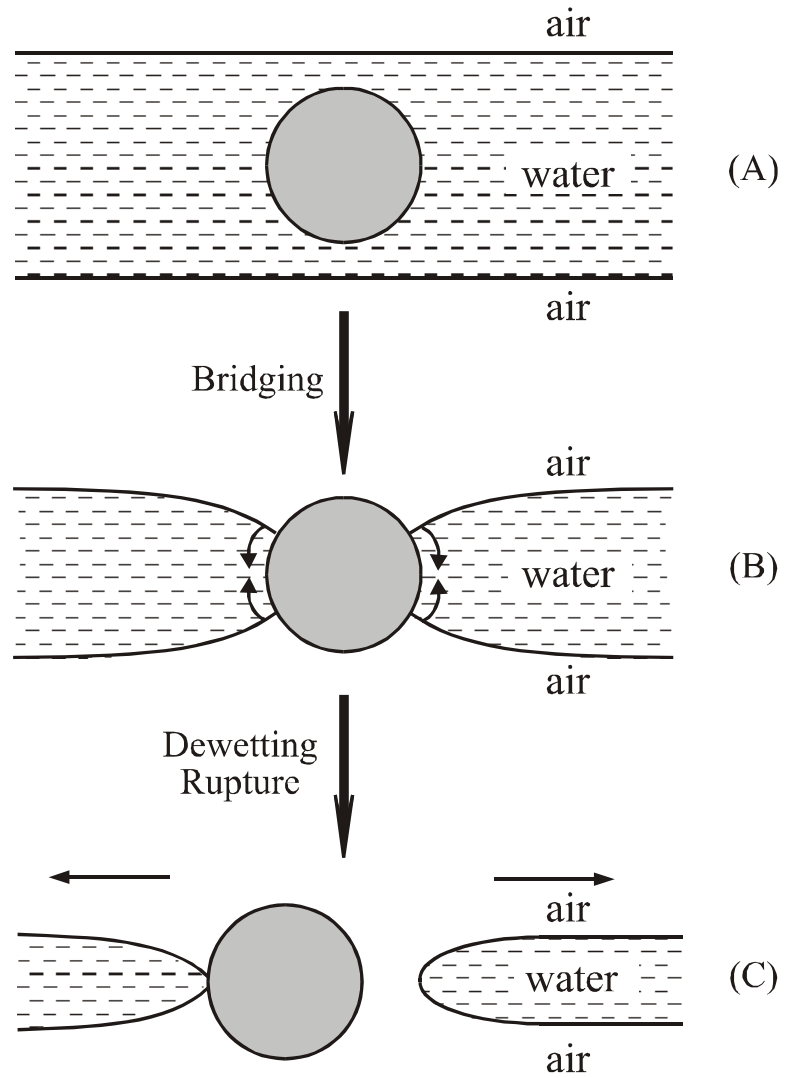
air

water   (A)

air

Bridging

air

water   (B)

air

Dewetting
Rupture

air

water   (C)

air

Figure 9. Schematic presentation of the bridging-dewetting mechanism of foam film rupture by hydrophobic solid particles [131, 139-141].
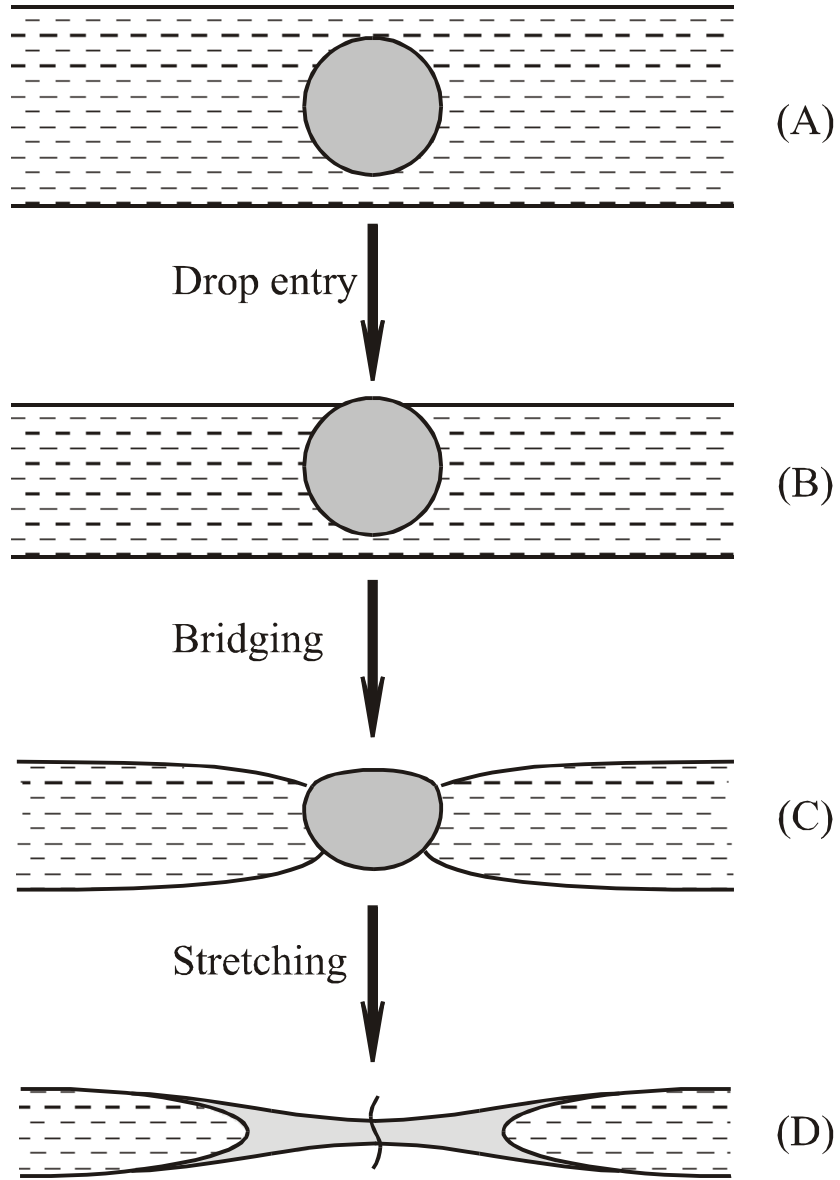
Figure 10. **"Bridging-stretching" mechanism of foam film destruction by a mixed oil-silica antifoam globule [137, 147]. After an oil bridge is formed (A→C), it stretches due to uncompensated capillary pressures at the oil-water and oil-air interfaces (C→D). Finally, the oil bridge ruptures in its thinnest central region (the vertical wavy line in D).**